Direct Observation of the Optical Anisotropy of the Holmium Nucleus

E. AMBLER, E. G. FULLER, AND H. MARSHAK
National Bureau of Standards, Washington, D. C.
(Received 9 November 1964)

The optical anisotropy of the holmium nucleus in the giant-resonance energy region has been shown to exist by measuring the yield of photoneutrons as a function of the orientation of the nucleus with respect to a bremsstrahlung beam direction. The nuclei were aligned by the Bleaney method using a continuously operating He^3 refrigerator to cool a single crystal of holmium ethyl sulfate to 0.29°K. The orientation effects observed could be explained if the absorption cross section for holmium was made up primarily of a component given by the dynamic collective theory, but also included a small scalar component (about 15% of the total) which had no orientation effects associated with it. In fitting the data, a reanalysis of previous data on the holmium absorption cross section was made.

I. INTRODUCTION

THE theory of Danos[1] and Okamoto[2] for the nuclear photoeffect in nuclei having large intrinsic deformations implies that the photon-absorption cross section for these nuclei depends upon the orientation of the nucleus with respect to the photon beam. This implication is also inherent in the recently postulated dynamic collective theory of the nuclear photoeffect developed by Danos, Greiner, and Kohr.[3,4] The first actual suggestion that the nucleus may be optically anisotropic was probably made by Baldin.[5] He pointed out that the magnitude of this effect was model-dependent and that the Danos-Okamoto model implied a large tensor polarizability or forward-scattering amplitude for those nuclei having a large intrinsic deformation. Subsequently, measurements made of the photon-scattering cross sections for tantalum[6] and holmium,[7,8] when interpreted in terms of their neutron-production cross sections, indicated the existence of a tensor-scattering amplitude for these nuclei that could be consistent with that predicted by the Danos-Okamoto model. The magnitude of the tensor-scattering-amplitude term in the scattering cross section for these nuclei is, however, in some doubt[8,9] as a result of possible systematic uncertainties in the magnitudes of both the scattering and neutron-production cross sections.

The object of the experiment to be described in this paper was to show directly that the holmium nucleus has a large intrinsic tensor scattering amplitude. This was done by showing that the photoneutron yield depended upon the orientation of the nuclear spin with respect to the photon-beam direction. In the following section, a brief discussion is given of the nuclear scattering amplitude and the consequences of its tensor character. In Sec. III the orientation of holmium in a single crystal of holmium ethyl sulfate by the Bleaney method is discussed. Section IV contains a general description of the experimental arrangement. The experimental procedure and results are presented in Sec. V, and the conclusions in Sec. VI.

II. THE NUCLEAR SCATTERING AMPLITUDE

It has been pointed out previously that the nuclear scattering and absorption cross sections for photons can be related by means of the forward scattering amplitude.[10] The relation between these cross sections is unique only when the scattering amplitude is a pure scalar quantity. The general case has been discussed by Placzek and by Fano.[11] For unoriented nuclear systems and electric dipole transitions, the tensor character of the scattering amplitude manifests itself by the appearance in the differential scattering cross section of terms in addition to the usual $(1+\cos^2\theta)$ term.[6,7] A direct consequence of this tensor character is a dependence of the photon-absorption cross section on the nuclear orientation with respect to the photon-beam direction. The magnitude of these effects in the absorption and scattering cross sections is model dependent. It is the purpose of this section to present the relationship in the context of the Danos-Okamoto model for the nuclear photoeffect in deformed nuclei as recently extended by Danos and Greiner.[3]

The photon scattering process in which a nucleus makes a transition from an initial state $|i\rangle$ to a final state $|f\rangle$ by means of the absorption of a photon of energy E_1, propagation vector $\mathbf{k}_1$, polarization q_1, and the emission of a photon of energy E_2, propagation

[1] M. Danos, Nucl. Phys. **5**, 23 (1958).
[2] K. Okamoto, Progr. Theoret. Phys. (Kyoto) **15**, 75 (1956); Phys. Rev. **110**, 143 (1958).
[3] M. Danos and W. Greiner, Phys. Rev. **134**, B284 (1964); Proceedings of the International Nuclear Physics Congress, Paris, 1964 (to be published); M. Danos and W. Greiner, Phys. Letters **8**, 113 (1964).
[4] M. Danos, W. Greiner, and C. B. Kohr (to be published).
[5] A. M. Baldin, Proceedings of the All Union Conference on Low and Medium Energy Nuclear Reactions (Akademiia Nauk, Moscow, 1957), p. 479; Nucl. Phys. **9**, 237 (1958).
[6] E. G. Fuller and E. Hayward, Phys. Rev. Letters **1**, 1507 (1958).
[7] E. G. Fuller and E. Hayward, Nucl. Phys. **30**, 613 (1962); Nucl. Phys. **37**, 176 (1962).
[8] P. A. Tipler, P. Axel, N. Stein, and D. C. Sutton, Phys. Rev. **129**, 2096 (1963).
[9] R. L. Bramblett, J. T. Caldwell, G. F. Auchampaugh, and S. C. Fultz, Phys. Rev. **129**, 2723 (1963).
[10] E. G. Fuller and E. Hayward, Phys. Rev. **101**, 692 (1956).
[11] G. Placzek, Marx Handbuch der Radiologie, (Akademische Verlagsgesellschaft, Leipzig, 1934) Vol. 6, Part 2, p. 303; U. Fano, Natl. Bur. Std. (U. S.) Technical Note No. 83, 1960 (unpublished).

vector $\mathbf{k}_2$, and polarization q_2, can be described by means of a scattering amplitude R_{21}. In second-order perturbation theory, this amplitude is given by

$$R_{21}=\sum_n\left[\frac{\langle f|H'(q_2,\mathbf{k}_2,\mathbf{r})^*|n\rangle\langle n|H'(q_1,\mathbf{k}_1,\mathbf{r})|i\rangle}{E_n-E_1-i\Gamma_n/2}+\frac{\langle f|H'(q_1,\mathbf{k}_1,\mathbf{r})|n\rangle\langle n|H'(q_2,\mathbf{k}_2,\mathbf{r})^*|i\rangle}{E_n+E_2+i\Gamma_n/2}\right], \quad (1)$$

where $H'(q_1,\mathbf{k}_1,\mathbf{r})$ and $H'(q_2,\mathbf{k}_2,\mathbf{r})^*$ describe the absorption of photon one and the emission of photon two. These terms arise from the multipole tensor expansion of the interaction of a plane wave with the nucleus. It is assumed that the plane wave is circularly polarized with respect to its propagation vector. The quantity Γ_n describes the damping of the intermediate state. The coherent forward scattering amplitude R_c is obtained by making the substitutions $|f\rangle=|i\rangle$, $E_1=E_2$, $\mathbf{k}_1=\mathbf{k}_2$ and $q_1=q_2$ in this expression. Assuming axially symmetric nuclear orientation, the absorption cross section is then given by the optical theorem

$$\sigma_a=4\pi\lambda\sum_{m_i}a_{m_i}\,\mathrm{Im}R_c\langle q,m_i\rangle_{\mathrm{av}}, \quad (2)$$

where a_{m_i} gives the population of the magnetic substate m_i, $(\sum_{m_i}a_{m_i}=1)$. For an unoriented nuclear system $a_{m_i}=1/(2I_i+1)$, where I_i is the angular momentum of the nuclear ground state. The angular brackets denote an average over q.

In the long-wavelength limit, the interaction operator is given by[12]

$$H'(q,\mathbf{k},\mathbf{r})=-\sum_{LM}\frac{i^Lk^L}{(2L-1)!!}\left(\frac{L+1}{2L}\right)^{1/2}\mathfrak{D}_{Mq}{}^L(R)N_M{}^L, \quad (3)$$

where

$$N_M{}^L=(Q_{LM}+Q'_{LM})-iq(M_{LM}+M'_{LM}).$$

The quantities Q_{LM} and Q'_{LM} represent, respectively, the charge and spin contributions of parity $(-1)^L$ resulting in electric transitions while M_{LM} and M'_{LM} represent the corresponding contributions of parity $(-1)^{L+1}$ resulting in magnetic transitions. The rotation R is from the beam axis to the quantization axis of the system. Making the above substitutions into Eq. 1, we obtain

$$R_c(q,m_i)=\sum_n\sum_{LM}\frac{k^{2L}}{[(2L-1)!!]^2}\left(\frac{L+1}{2L}\right)\mathfrak{D}_{Mq}{}^L\mathfrak{D}_{Mq}{}^{L*}\times\left[\frac{\langle I_im_i\alpha_i|N_M{}^{L*}|I_nm_n\alpha_n\rangle\langle I_nm_n\alpha_n|N_M{}^L|I_im_i\alpha_i\rangle}{E_n-E-i\Gamma_n/2}+\frac{\langle I_im_i\alpha_i|N_M{}^L|I_nm_n\alpha_n\rangle\langle I_nm_n\alpha_n|N_M{}^{L*}|I_im_i\alpha_i\rangle}{E_n+E+i\Gamma_n/2}\right]. \quad (4)$$

The quantity α denotes quantum numbers other than I and m required to specify a given nuclear state. Note that interference terms do not occur. Using the phase conventions of Ref. 12, we make use of the following relations:

$$N_M{}^{L*}=(-1)^{M-1}N_{-M}{}^L$$

$$\langle I_im_i\alpha_i|N_M{}^L|I_nm_n\alpha_n\rangle=(-1)^{2L}\langle I_nm_nLM|I_im_i\rangle\times\langle I_i\alpha_i\|\mathbf{N}^L\|I_n\alpha_n\rangle$$

$$\langle I_i\alpha_i\|\mathbf{N}^L\|I_n\alpha_n\rangle=(-1)^{I_i-I_n-1}\left(\frac{2I_n+1}{2I_i+1}\right)^{1/2}\times\langle I_n\alpha_n\|\mathbf{N}^L\|I_i\alpha_i\rangle^*$$

$$\mathfrak{D}_{Mq}{}^L\mathfrak{D}_{Mq}{}^{L*}=(-1)^{M-q}\sum_\nu\langle L-qLq|\nu0\rangle\times\langle L-MLM|\nu0\rangle P_\nu(\cos\theta),$$

and obtain

$$R_c(q,m_i)=\sum_n\sum_L\frac{k^{2L}}{[(2L-1)!!]^2}\left(\frac{L+1}{2L}\right)|\langle I_n\alpha_n\|\mathbf{N}^L\|I_i\alpha_i\rangle|^2(-1)^{I_i-I_n+q}\left(\frac{2I_n+1}{2I_i+1}\right)^{1/2}\sum_\nu\langle L-qLq|\nu0\rangle P_\nu(\cos\theta)\times\left[\frac{1}{E_n-E-i\Gamma_n/2}+\frac{(-1)^\nu}{E_n+E+i\Gamma_n/2}\right]\sum_M\langle L-MLM|\nu0\rangle\langle I_nm_nL-M|I_im_i\rangle\langle I_im_iLM|I_nm_n\rangle. \quad (5)$$

The dependence on photon polarization is given by the Clebsch-Gordan coefficient $\langle L-qLq|\nu0\rangle$. Since in our case the incident beam is not circularly polarized and $\langle L-qLq|\nu0\rangle=(-1)^\nu\langle LqL-q|\nu0\rangle$, terms with odd ν will be identically zero.

We can contract the summation over M in Eq. (5) into a $6-j$ symbol multiplied by a Clebsch-Gordan coefficient. Putting this into Eq. (2), and introducing the nuclear orientation parameters for axial symmetry,[13]

$$\bar{f}_\nu(T)=\sum_{m_i}a_{m_i}(-1)^{I_i-m_i}\langle I_im_iI_i-m_i|\nu0\rangle.$$

We obtain

$$\sigma_a(E,T,\theta)=\sum_{\nu\ \mathrm{even}}\bar{f}_\nu(T)\sigma_\nu(E)P_\nu(\cos\theta), \quad (6a)$$

[12] D. M. Brink and G. R. Satchler, *Angular Momentum* (Oxford University Press, Oxford, 1962).
[13] H. A. Tolhoek and J. A. M. Cox, Physica **19**, 101 (1953).

where

$$\sigma_\nu(E)=4\pi\lambda\sum_L\frac{k^{2L}}{[(2L-1)!!]^2}\left(\frac{L+1}{2L}\right)\langle L-1L1\,|\,\nu0\rangle\sum_n|\langle I_n\alpha_n\|\mathbf{N}^L\|I_i\alpha_i\rangle|^2$$
$$\times\frac{2E_nE\Gamma_n}{(E_n^2-E^2)^2+E^2\Gamma_n^2}(-1)^{I_i+I_n-1}(2I_n+1)\begin{Bmatrix}I_i & I_n & L\\ L & \nu & I_i\end{Bmatrix}. \quad (6b)$$

We note that $0\leq\nu\leq$ the smaller of $2L$ or $2I_i$. In writing $\bar{f}_\nu(T)$, we display the fact that the nuclear orientation depends only upon the temperature T of the sample. The orientation parameters $\bar{f}_\nu(T)$ are related to the more familiar $f_\nu(T)$ by the following expression:

$$\bar{f}_\nu(T)=f_\nu(T)\binom{2\nu}{\nu}I_i{}^\nu\left[\frac{(2\nu+1)(2I_i-\nu)!}{(2I_i+\nu+1)!}\right]^{1/2}.$$

Equation (6a) can be written

$$\sigma_a(E,T,\theta)=\sum_{\nu\text{ even}}f_\nu(T)\sigma_\nu'(E)P_\nu(\cos\theta), \quad (6c)$$

where $\sigma_\nu'(E)$ now includes the factor

$$\binom{2\nu}{\nu}I_i{}^\nu\left[\frac{(2\nu+1)(2I_i-\nu)!}{(2I_i+\nu+1)!}\right]^{1/2}.$$

Equation (6a) clearly separates the temperature, energy, and angular factors in the cross section through $\bar{f}_\nu(T)$, $\sigma_\nu(E)$, and $P_\nu(\cos\theta)$, respectively. The basic aim of the experiment reduces to demonstrating the existence of terms for which $\nu>0$.

The evaluation of the matrix elements in Eq. (6b) requires some model for the nuclear photoeffect. In the hydrodynamical model[1,2] the giant resonance results from an electric-dipole oscillation of neutrons against protons. Viewed from the standpoint of the collective model, the actual motion takes place in the intrinsic system. In terms of Cartesian coordinates, there is a dipole mode of excitation associated with each of the three axes. For a nucleus which is axially symmetric with respect to the z axis, the two modes associated with the x and y axes are degenerate and appear at the same energy. For a prolate shape the degenerate excitation occurs at a higher energy than the nondegenerate one. In a triaxial nucleus, the x and y axes are not equivalent and the degeneracy associated with these two axes disappears. Expanding these modes in spherical waves, the mode along the z axis has $\Delta K=0$, while each of the modes along the x and y axes are linear suppositions of $\Delta K=+1$ and $\Delta K=-1$. In the extension of the hydrodynamical model, Danos, Greiner, and Kohr[4] consider coupling of the dipole modes to rotations, surface vibrations, and single-particle motion. Qualitatively, the coupling results in a polarization of the axially symmetric nucleus into a triaxially shaped nucleus. Therefore, the giant resonance splits into three modes which are designated by the quantum number $S=0,\pm1$, where $S=0$ corresponds to the mode associated with the z axis, and ±1 to the modes associated with the x and y axes. Their detailed theory shows that, to a good approximation, stationary states can be taken to be suitably symmetrized combinations of a rotational part $\mathfrak{D}_{mK}{}^I$ and an intrinsic part $|\Omega KSn_0n_2\rangle$, where Ω is the projection of the odd-particle angular momentum on the intrinsic axis, and n_0 and n_2 are quantum numbers associated with the β and γ quadrupole vibrational modes, respectively. It is found that only the $S=\pm1$ dipole mode is appreciably affected, and this mode is split through coupling with the γ vibrations. The single-particle motion plays no essential part, and Ω, which is equal to K_i and I_i in the ground state, remains a constant.

As in the simple picture, therefore, the motion can be "projected out" onto the spin axis, and the reduced matrix elements of Eq. (6b) can be written in terms of the matrix elements in the intrinsic system. This is done by introducing operators $\tilde{N}_{M'}{}^L$ through the transformation,

$$N_M{}^L=\sum_{M'}\mathfrak{D}_{MM'}{}^L\tilde{N}_{M'}{}^L.$$

These intrinsic operators are then introduced into the reduced matrix elements together with the detailed form of the stationary states, and integration of these three $\mathfrak{D}$ functions is performed over rotational coordinates. We then obtain, dropping quantum numbers which do not change,

$$\langle I_nK_nSn_2\|\mathbf{N}^L\|I_iK_i\rangle$$
$$=\left(\frac{2I_i+1}{2I_n+1}\right)^{1/2}\langle I_iK_iL\Delta K\,|\,I_nK_n\rangle\langle K_nSn_2|\tilde{N}_{\Delta K}{}^L|\,K_i\rangle,$$

where $\Delta K=K_n-K_i$. Thus,

$$\sigma_\nu(E)=4\pi\lambda\sum_L\frac{k^{2L}}{[(2L-1)!!]^2}\left(\frac{L+1}{2L}\right)\langle L-1L1\,|\,\nu0\rangle\sum_{K_nSn_2}|\langle K_nSn_2|\tilde{N}_{\Delta K}{}^L|\,K_i\rangle|^2$$
$$\times\frac{2E_{K_nSn_2}E\Gamma_{K_nSn_2}}{(E_{K_nSn_2}{}^2-E^2)^2+E^2\Gamma_{K_nSn_2}{}^2}\sum_{I_n}(-1)^{I_i+I_n-1}(2I_n+1)\begin{Bmatrix}I_i & I_n & L\\ L & \nu & I_i\end{Bmatrix}\langle I_iK_iL\Delta K\,|\,I_nK_n\rangle^2\left(\frac{2I_i+1}{2I_n+1}\right).$$

The matrix elements can be brought outside the summation over I_n since they are completely defined by the internal quantum numbers. Although there is a dependence of the $E_{K_nSn_2}$'s and the $\Gamma_{K_nSn_2}$'s on I_n, this is small, being of the order of the rotational energy; so we may neglect it and bring the resonance term outside of the summation over I_n. The summation over I_n reduces to

$$(-1)^{\Delta K+1}\left(\frac{2I_i+1}{2\nu+1}\right)^{1/2}\langle I_iK_i\nu 0|I_iK_i\rangle\langle L\Delta KL-\Delta K|\nu 0\rangle.$$

The complete expression for $\sigma_\nu(E)$ is

$$\sigma_\nu(E)=4\pi\lambda\sum_L\frac{k^{2L}}{[(2L-1)!!]^2}\left(\frac{L+1}{2L}\right)\langle L-1L1|\nu 0\rangle\sum_{K_nSn_2}|\langle K_nSn_2|\tilde{N}_{\Delta K}{}^L|K_i\rangle|^2$$
$$\times\frac{2E_{K_nSn_2}E\Gamma_{K_nSn_2}}{(E_{K_nSn_2}{}^2-E^2)+E^2\Gamma_{K_nSn_2}{}^2}(-1)^{\Delta K+1}\left(\frac{2I_i+1}{2\nu+1}\right)^{1/2}\langle I_iK_i\nu 0|I_iK_i\rangle\langle L\Delta KL-\Delta K|\nu 0\rangle. \quad (7)$$

Substituting this into Eq. (6a), we obtain the absorption cross section for an unpolarized beam evaluated explicitly in terms of the dynamic collective model.

$$\sigma_a(E,\theta,T)=\sum_{\nu\text{ even}}f_\nu(T)\sigma_\nu'(E)P_\nu(\cos\theta), \quad (8a)$$

where

$$\sigma_\nu'(E)=\sum_L\sigma'_{L,\nu}(E) \quad (8b)$$

$$\sigma'_{L,\nu}(E)=\binom{2\nu}{\nu}I_i{}^\nu\left[\frac{(2I_i+1)(2I_i-\nu)!}{(2I_i+\nu+1)!}\right]^{1/2}$$
$$\times\langle I_iK_i\nu 0|I_iK_i\rangle\langle L1L-1|\nu 0\rangle$$
$$\times\sum_{\Delta K}(-1)^{\Delta K+1}\langle L\Delta KL-\Delta K|\nu 0\rangle\sigma'_{L,\nu,\Delta K}, \quad (8c)$$

and

$$\sigma'_{L,\nu,\Delta K}=4\pi\lambda\frac{k^{2L}}{[(2L-1)!!]^2}\left(\frac{L+1}{2L}\right)$$
$$\times\sum_{Sn_2}\frac{2E_{K_nSn_2}E\Gamma_{K_nSn_2}}{(E_{K_nSn_2}{}^2-E^2)+E^2\Gamma_{K_nSn_2}{}^2}$$
$$\times|\langle K_nSn_2|\tilde{N}_{\Delta K}{}^L|K_i\rangle|^2. \quad (8d)$$

III. NUCLEAR ALIGNMENT OF Ho^{165}

Large values of nuclear alignment of Ho^{165} can be obtained by the Bleaney method[14] using single crystals of holmium ethyl sulfate or holmium metal. Although the salt, $Ho(C_2H_5SO_4)_3\cdot 9H_2O$, contains only about 23% of holmium by weight, it was preferred over holmium metal for this experiment for a number of reasons. At the outset of this work, the salt was much more readily available in the form of large single crystals. Furthermore, the orientation effects would be larger with the salt since all the holmium ions occupy equivalent sites[15,16] resulting in the alignment of all nuclei with respect to a common crystallographic direction, taken to be the z axis in what follows. In the metal, in zero field, the spiral configuration[17] of the atomic moments gives rise to more than one equivalent direction. Although large alignments can be obtained for each system of nuclei whose atomic moments are along these directions, the average alignment for the entire sample is considerably reduced when compared to the salt. This net alignment in the metal can be increased by the application of an external field along one of the easy directions of magnetization. A value of about 10 kOe is needed in order to get close to complete saturation of the atomic moments.[18] This should be contrasted with the situation for the salt where no external field is necessary.

The explicit form of the nuclear alignment parameter f_2 is

$$f_2=I^{-2}[\sum_m m^2a_m-\tfrac{1}{3}I(I+1)], \quad (9)$$

where I is the nuclear spin, m labels the eigenstates of I_z, and a_m are the populations of these states. The nuclear alignment for the salt is calculated from the low-temperature magnetic properties which have been measured by paramagnetic-resonance techniques.[15,16] Stated briefly, the conclusions of these measurements are that the crystal field splits the $4f^{10}$, $^5I_8$ configuration of the Ho^{3+} ion in such a way that at very low temperatures only a doublet state is populated. This doublet can then be described by an effective electron spin $S=\frac{1}{2}$ state with spin Hamiltonian,[15]

$$\mathcal{H}=g_{11}\beta S_zH_z+AS_zI_z+\Delta_xS_x+\Delta_yS_y. \quad (10)$$

The first term describes the effect of an applied external magnetic field, β being the Bohr magneton.

[14] B. Bleaney, Phil. Mag. **42**, 441 (1951).

[15] J. M. Baker and B. Bleaney, Proc. Phys. Soc. (London) **A68**, 1090 (1955).

[16] J. M. Baker and B. Bleaney, Proc. Roy. Soc. (London) **A245**, 156 (1958).

[17] W. C. Koehler, J. Appl. Phys. **32**, 20S (1961).

[18] D. L. Strandburg, S. Legvold, and F. H. Spedding, Phys. Rev. **127**, 2046 (1962).

The value of the parallel g factor $g_{\parallel}$ is 15.36, while the perpendicular g factor $g_{\perp}$ is zero. Since there is symmetry about the z axis the x and y directions need not be specified more exactly. The second term is the most relevant and describes the magnetic hyperfine splitting (hfs). The value of the hfs constant A/k is 0.480°K, where k is Boltzmann's constant. Since the ground state is not a Kramers doublet the terms in Δ_x and Δ_y are included to take into account the observed splittings of the $S=\frac{1}{2}$ state arising from the effects of the crystal electric field. These observed splittings are not sharp but cover a range of values, and are attributed to random local distortions in the crystal field from the predominant symmetry. On solving the secular equation appropriate to the above spin Hamiltonian, it is found that the only quantity affecting the energy levels is $\Delta=(\Delta_x^2+\Delta_y^2)^{1/2}$, and the resonance results can be fitted to a distribution of values of Δ of the form

$$e^{-x^2}xdx, \tag{11}$$

where $x=(\Delta/\Delta_0)$, and the constant $\Delta_0=0.093$°K.

A word of caution should be said concerning this procedure. The values of the above constants[15,16] were obtained using a magnetically dilute salt, viz., yttrium ethyl sulfate, with about 1% of the yttrium ions replaced by holmium, while the present experiments were done on the concentrated holmium salt. The question arises to what extent we are justified in assuming the same spin Hamiltonian and parameters for the concentrated salt. It might have been supposed, for example, that the crystal field distortions in the more homogeneous concentrated salt would be less than in the dilute salt, and that, therefore, Δ_0 would be less. In the case of the praeseodimium salt, however (Pr^{3+} is also a non-Kramers ion), the evidence[19] from magnetic and thermal measurements show Δ_0 to be almost three times greater in the concentrated salt. Even such an increase in Δ_0 in the case of the holmium salt would have a negligible effect on the calculated value of f_2, on account of the very large diagonal terms in A. In fact, even if Δ_0 is as large as A, the effect would be to lower f_2 only by about 5% at our operating temperature. In order for f_2 to be seriously affected, Δ must be about equal to IA. Very rough magnetic susceptibility measurements made at this laboratory indicate that such is not the case, although no reliable estimates of Δ_0 could be made because of the complicating effects of other factors affecting the magnetic susceptibility. Recent unpublished specific-heat measurements[20] of the Clarendon Laboratory on concentrated holmium ethyl sulfate indicate that the value of Δ_0 is not much more than twice the value for the dilute salt.

The energy levels for the Hamiltonian given in Eq. (10) are

$$W_m=\pm\tfrac{1}{2}[(g_{\parallel}\beta H+mA)^2+\Delta^2]^{1/2}. \tag{12}$$

The presence of Δ mixes eigenstates of S_z. With the relative values of A and Δ given above, the A term dominates, and in zero external field we have essentially a pattern of equally spaced hyperfine doublets, with quantum numbers $\pm m$. The populations a_m are determined by the Boltzmann factor, $e^{-W_m/kT}$, and the value of f_2 as a function of temperature is then easily calculated. The result is shown in Fig. 1. As a result of the large hfs, the nuclear alignment is considerable, even at temperatures around 0.3°K. This allowed a relatively simple and flexible apparatus to be designed using a He^3 refrigerator with, essentially, continuous operation.

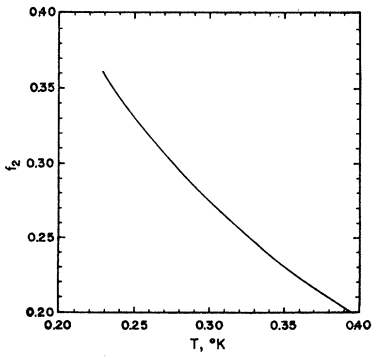

FIG. 1. Nuclear orientation parameter f_2 as a function of temperature for Ho^{165}. The quantity f_2 was calculated for holmium nuclei in a single crystal of holmium ethyl sulfate.

IV. EXPERIMENTAL ARRANGEMENT

A schematic over-all view of the experimental arrangement is shown in Fig. 2. The bremsstrahlung beam, generated in the betatron's internal target, was collimated and then passed through the transmission ionization-chamber monitor before entering the horizontal evacuated tube which passed through the neutron detector. This horizontal tube was an integral part of the He^3 refrigerator, i.e., the main Dewar vacuum extended outside of the neutron detector to the 0.00625 cm aluminum windows at the ends of this tube. As is

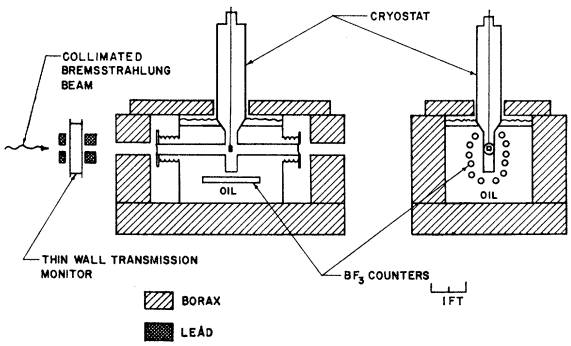

FIG. 2. Experimental arrangement.

[19] H. Meyer, Phys. Chem. Solids 9, 296 (1959).

[20] Dr. A. H. Cooke (private communication).

indicated in Fig. 2, the main body of the refrigerator was above the beam tube. The holmium ethyl sulfate crystal was attached to a long, thin-walled stainless steel tube that passed out through the top of the apparatus. By means of this tube, it was possible to both raise the crystal out of the bremsstrahlung beam as well as rotate the axis of nuclear alignment to any angle with respect to the beam direction without stopping the operation of the refrigerator. The neutron detector and the crystal-refrigerator combination were lined up with respect to the beam axis by radiographic means. The final line up was carried out at low temperatures.

The neutron detector was a modified "Halpern-type." It consisted of twelve BF_3 proportional counters placed parallel to and symmetrically around the central beam tube. They were immersed in a mineral oil bath which served as the moderator. The twelve BF_3 counters were connected into three groups of four each for amplification, gating, and counting. These counters were so insensitive to x rays that for the intensities used in this experiment it was possible to open the gate before the x-ray beam pulse. The recorded events occurred in a 700-μsec period starting 10 μsec before the betatron's x-ray burst. The over-all efficiency of the detector, neglecting the gating effect, was 7.8%. This was determined by using calibrated RaBe (α,n) and RaDBe (α,n) sources. The ratio of the number of photoneutrons detected with the gates on to those detected with the gates off was 0.98. Further details of the detector will be described elsewhere.[21]

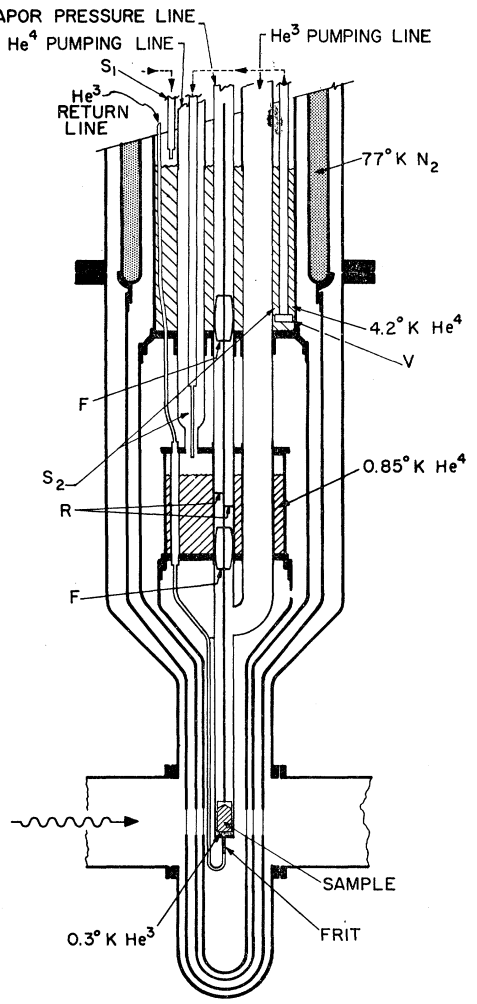

FIG. 3. Schematic view of He^3 refrigerator.

At the center of the neutron detector, i.e., in the region of the holmium ethyl sulfate crystal, the collimated bremsstrahlung beam was approximately 2.64 cm in diameter. In this region the beam passed through four 0.0038-cm aluminum windows, the 0.85°K radiation shield and the He^3 tail. At the beam level, the 0.85°K radiation shield was a 3.8-cm diam magnesium tube with 0.025-cm walls; the He^3 tail was a 2.22-cm diam stainless steel tube with 0.0127-cm walls. The backgrounds produced by these materials were determined by raising the crystal out of the beam.

The cryogenic features of the He^3 refrigerator have been fully described elsewhere,[22] so only a few salient points will be referred to here. A schematic view of the refrigerator is shown in Fig. 3. The He^3 tail contained the sample, the lower end of which was immersed in liquid He^3. The sample was attached to the long, thin-walled, stainless tube mentioned earlier, on which were located radiation shields, *R*, and centering devices *F*. A heater placed on the He^3 tail enabled the temperature of the sample to be raised so that the nuclear alignment could be destroyed without altering the position of the sample. The He^3 was pumped through the tube indicated (He^3 pumping line) and continuously recirculated (He^3 return line) to the condenser located in the 0.85°K bath where it was reliquefied. From there it passed through the porous plug (frit) back into the He^3 bath. The temperature of the He^3 was measured by means of its vapor pressure[23] transmitted through the tube indicated (vapor pressure line) to a McLeod gauge. Corrections were applied for thermomolecular pressure differences.[24] Since such corrections were rather large at the lowest operating temperature, a number of checks were made on the accuracy of this procedure. Both a carbon resistance thermometer and a paramagnetic salt obeying Curie's law were calibrated against the vapor pressure at higher temperatures were the thermomolecular pressure differences were small. At the lower temperatures, the temperature obtained from the corrected vapor pressure readings agreed with those obtained from the secondary thermometers to within about a

[21] H. Gerstenberg and E. G. Fuller (to be published).
[22] E. Ambler, R. B. Dove, and R. S. Kaeser, *Advances in Cryogenic Engineering* (Plenum Press, New York, 1963), Vol. 8, p. 443.
[23] S. G. Sydoriak and T. R. Roberts, Phys. Rev. **106**, 175 (1957).
[24] T. R. Roberts and S. G. Sydoriak, Phys. Rev. **102**, 304 (1956).

millidegree. It was also shown that in order to establish a sufficiently good thermal contact, the lower tip of the crystal had to be actually immersed in the liquid He^3. The lowest operating temperature of 0.29°K was found to be very stable during runs, and also reproducible from one run to the next.

V. EXPERIMENTAL PROCEDURE AND RESULTS

The experiment consisted of measuring the yield of photoneutrons from the 5.81-g holmium ethyl sulfate crystal for a series of six betatron operating energies. At each energy the yield was measured as a function of the orientation of the c axis of the crystal with respect to the bremsstrahlung beam direction. In terms of the cross sections defined by Eq. (6c) and of $\bar{\sigma}$, the average cross section per molecule for producing a neutron from the constituents of the crystal other than holmium, this yield $Y(E_i,T,\theta)$, is proportional to

$$\begin{aligned} Y(E_i,T,\theta) \approx & \int_0^{E_i} N(E,E_i) \\ & \times\{\bar{\sigma}(E)+M[\sigma_s'(E)+f_2(T)\sigma_2'(E)P_2(\cos\theta) \\ & +f_4(T)\sigma_4'(E)P_4(\cos\theta)]\}dE \\ = & y_s(E_i)+Y_s(E_i)+Y_t(E_i,T,\theta). \end{aligned} \tag{13}$$

The quantity $N(E,E_i)$ is the bremsstrahlung spectrum, M is the neutron multiplicity for holmium, θ is the angle between the c axis of the crystal and the beam direction, σ_s' is used instead of σ_0' for the scalar cross section, and $\bar{\sigma}$ is given by

$$\bar{\sigma}=6\sigma(\mathrm{C})+21\sigma(\mathrm{O})+3\sigma(\mathrm{S}), \tag{14}$$

where $\sigma(\mathrm{C})$, $\sigma(\mathrm{O})$, and $\sigma(\mathrm{S})$ represent the cross sections for the production of photoneutrons for carbon, oxygen, and sulfur, respectively. The assumption was made that the neutron production cross section for holmium accounts for the total absorption cross section. This is a good approximation for such a heavy nucleus. As a result of the high (γ,n) thresholds and the small neutron production cross sections of the other constituents in the crystal, the contribution from the term containing $\bar{\sigma}$, $y_s(E_i)$, was small compared to that from the terms containing the holmium cross section. At 20 MeV, the calculated yield from the $\bar{\sigma}$ term was only 4.6% of the holmium yield. Below 16 MeV this yield was completely negligible.

At each energy E_i, the quantity $Y(E_i,T,\theta)$ was measured for the two angles for which $P_2(\cos\theta)$ is a maximum, the two for which it is a minimum and with the exception of 14.52 MeV, the four angles for which $P_2(\cos\theta)$ is 0. Measurements were made at a temperature of 0.29°K as well as at temperatures of 4.2 and 77°K. In general, a given day's measurements were taken with the crystal at a fixed temperature and with the betatron operating at one of the six energies. The procedure followed was to make a 20 to 25 min run at a given angle, rotate to the next angle and make another run. The sequence of angles measured was 0°, 54.8°, 90°, etc. around the full 360° range. The angular scale was actually established during some of the first runs by adjusting the zero until the measured yields were the same at 54.8°, 125.2°, 134.8°, and 305.2°. In a typical day's running each angle was measured about three times. At the lowest bremsstrahlung energy the yield was determined with a statistical uncertainty of ±3.2% as given by the square root of the number of counts observed in a single run. The corresponding figure at 20 MeV was ±0.31%. When the neutron yields at a given energy and temperature were grouped into the three angle groups ($P_2=1$, $P_2=-\frac{1}{2}$, $P_2=0$), the data in any group were consistent within the statistical uncertainties in the individual measurements. Backgrounds were determined at each operating energy by raising the crystal out of the bremsstrahlung beam. This background was produced predominantly by the beam passing through the various radiation shields and tails of the refrigerator. It accounted for 23% of the counts observed at 10 MeV and 42% of those observed at 20 MeV.

From these measurements the following experimental quantities were determined for each of the six betatron energies used in this experiment:

At 4.2°K and 70°K,

$$\begin{aligned} Y_s(E_i) &= Y_W(E_i,\ P_2=1)-\text{background}, \\ \Delta Y_W(E_i) &= Y_W(E_i,\ P_2=-\tfrac{1}{2})-Y_W(E_i,\ P_2=1). \end{aligned}$$

The subscript W on the yield Y refers to target warm, i.e., to either of the above temperatures, and corresponds to nuclei randomly oriented. The subscript c used below refers to target cold, i.e., 0.29°K and corresponds to nuclei aligned.

At 0.29°K,

$$\begin{aligned} \Delta Y_c(E_i) &= Y_c(E_i,\ P_2=-\tfrac{1}{2})-Y_c(E_i,\ P_2=1), \\ \delta Y_c(E_i) &= Y_c(E_i,\ P_2=0)-Y_c(E_i,\ P_2=1), \\ R_1 &= \Delta Y_c(E_i)/\delta Y_c(E_i), \\ R_2 &= \Delta Y_c(E_i)/[Y_s(E_i)-y_s(E_i)]. \end{aligned} \tag{15}$$

For each of the energies at which data were taken the quantity $Y_s(E_i)$ was calculated from the Ho, S, C, and O neutron-production cross sections and the absolute response function of the ionization chamber monitor. Since the ratio of the crystal area to the beam area was not known very accurately, it was not possible to make a direct comparison of the calculated and measured absolute yields. The ratio of these two quantities, however, was constant for the six energies at which measurements were made to within the estimated overall uncertainties in the calculated yields of about 2%. This was taken as an indication that the mean neutron detection efficiency did not vary markedly with brems-

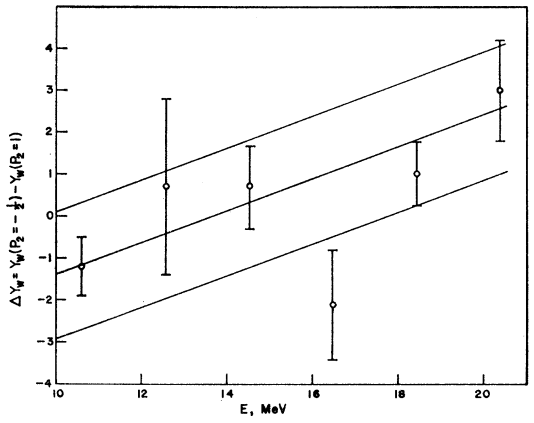

FIG. 4. Asymmetry of photoneutron yield measured at 77°K. Statistical uncertainties as determined from the square root of the number of counts observed at each energy are indicated in the individual points. The abscissa represents the peak energy of the bremsstrahlung spectrum.

strahlung energy in spite of the presence of the refrigerator system within the moderating material.

In Fig. 4, the quantity $\Delta Y_W(E_i)$ is given as a function of E_i. This quantity would be zero at all energies if the holmium ethyl sulfate crystal were symmetrical with respect to the axis of rotation. The crystal used was not perfectly symmetrical about this axis. The calculated asymmetry in the neutron yield resulting from the difference in the photon absorption in the crystal for the two orientations was 0.5%. In Fig. 4, the point at about 20 MeV corresponds to an asymmetry of about 0.2%. It was assumed that this discrepancy resulted from a slight nonuniformity in the bremsstrahlung beam across its diameter. This nonuniformity could be produced by attenuation of the beam in the cylindrical walls of the refrigerator. All of the data taken at 0.29°K were corrected for this asymmetry. The correction made and its assumed uncertainty was that given by the straight lines in Fig. 4. The uncertainty in this correction contributed the major part of the uncertainties given for the final results.

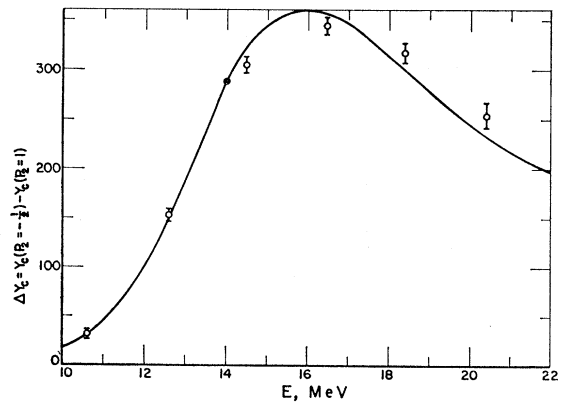

FIG. 5. Asymmetry of photoneutron yield measured at 0.29°K. The root mean square errors determined from the estimated uncertainties in the asymmetry measured at 77°K and the rms deviation of the measurements at 0.29°K are indicated in the experimental points. The abscissa represents the peak energy of the bremsstrahlung spectrum.

In Fig. 5, the quantity $\Delta Y_c(E_i)$, corrected for $\Delta Y_W(E_i)$, is given as a function of E_i. The ordinate scale in this figure is in the same units as that used in Fig. 4. Since there are no orientation effects present in the background or the yields represented by $y_s(E_i)$ and $Y_s(E_i)$ in Eq. (13), the quantity $\Delta Y_c(E_i)$ is directly related to the terms dependent on σ_2' and σ_4'. No background corrections have to be made in determining the magnitude of this quantity. That the σ_2' term contributes the major part of the orientation effect is shown in Fig. 6, where the ratio R_1 is plotted. This ratio should be exactly 1.5 if only the σ_2' term is present in Eq. (13). As a scale factor, if the coefficient of the P_4 term were 8% of that of the P_2 term, the ratio would be 1.4. The fact that the measured values of R_1 are all 1.5 within the experimental uncertainties is a direct confirmation of the dipole character of the tensor scattering amplitude of the holmium nucleus. This is not a very critical test since, as can be seen from Eq. (6a), quadrupole transitions would also result in a P_2 term. It would be necessary for the quadrupole strength to be very large and have a very favorable distribution in energy if it were to be seen in an integral experiment of this type.

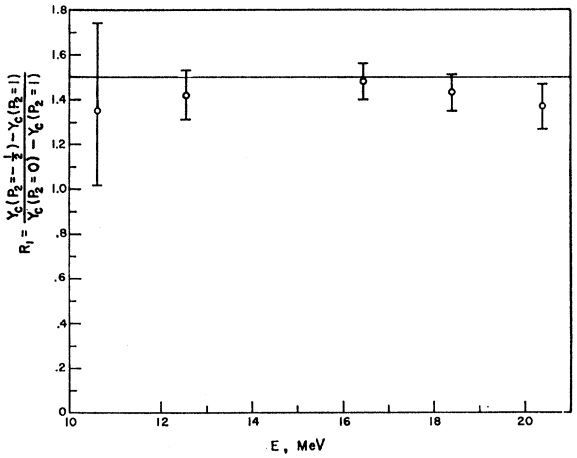

FIG. 6. Dependence of photoneutron yield asymmetry on the angle between the photon-beam direction and the nuclear alignment axis. The uncertainties indicated in the experimental points are defined in the caption for Fig. 5. The line at 1.5 is the value expected for a pure $P_2(\cos\theta)$ dependence of the alignment effect. The ordinate represents the peak energy of the bremsstrahlung spectrum.

In Fig. 7, the quantity R_2 is plotted as a function of peak bremsstrahlung energy. This quantity is the yield curve for the orientation dependent part of the cross section normalized in terms of the yield resulting from the scalar holmium cross section. As a result of the difficulties mentioned earlier in determining an absolute

cross section, it is felt that these data give the best indication of the magnitude of orientation-dependent cross section that can be obtained from this experiment.

VI. CONCLUSIONS AND DISCUSSION

The results of this experiment, as well as those of a previous measurement of the giant resonance for holmium,[7] have been compared with the predictions of the dynamic collective theory of the nuclear photoeffect as postulated by Danos and Greiner.[3] In this theory the beta and gamma vibrations of the nuclear ground state couple with the dipole modes responsible for the giant resonance resulting in a splitting of the high-energy mode into two main peaks and two smaller statellites. The magnitude of this splitting depends directly upon the energies of the ground state beta and gamma vibrations as well as on the deformation parameter β_0.

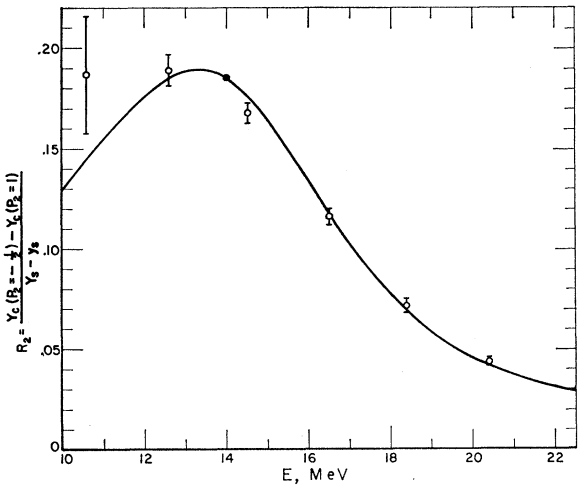

FIG. 7. Asymmetry of photoneutron yield normalized in terms of the orientation-independent yield. The uncertainties indicated in the experimental points are defined in the caption for Fig. 5. The abscissa represents the peak energy of the bremsstrahlung spectrum.

In the intrinsic system there are four eigenvalues associated with transitions in which oscillations are induced perpendicular to the nuclear symmetry axis and only one associated with oscillations along this axis.

In Fig. 8, the data for holmium previously measured in this laboratory have been replotted. There are several differences between the data plotted in Fig. 8 and those given in Fig. 4 of Ref. 7. It was found that the points at 13.5 and 14.5 MeV in the old data had been incorrectly determined from the raw experimental data. The correct values are given in Fig. 8. The second correction has to do with the magnitude of the cross sections plotted. A recent study[21] made of the neutron detection efficiency for a "Halpern-type" detector has shown that the neutron production cross sections given in Ref. 7 should be reduced by a factor of 0.69. A third difference is in the corrections made for the neutron multiplicity. One

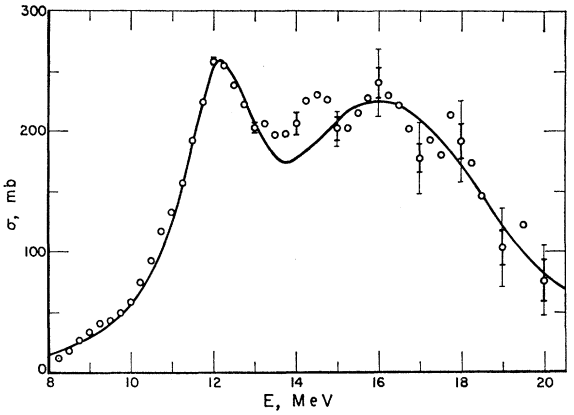

FIG. 8. Photoneutron-producing cross section for Ho^{165} as a function of photon energy. The points above 14.25 MeV have been corrected for neutron multiplicity. Horizontal bars represent typical statistical uncertainties in data points. Light extensions on the bars indicate the uncertainties in the multiplicity correction. The smooth curve is calculated from the theory of Danos and Greiner using the parameters given in Table I.

of the big uncertainties in the analysis of the previous data was the value for the threshold for the $(\gamma,2n)$ reaction. This has now been fairly well determined to be 14.25 MeV.[9] There are still considerable discrepancies in the magnitude of the $(\gamma,2n)$ cross section relative to the total neutron production cross section[9,25] so that while the threshold is better known, the multiplicity correction as a function of energy is still subject to some uncertainty. The data of Fig. 8 have been corrected for the neutron multiplicity by using a function based on the data of Carver and Turchinetz which depends only upon the energy above the $(\gamma,2n)$ threshold (curve "$C+T$" in Fig. 3 of Ref. 7). This curve falls between those derived from the two measurements made of the $(\gamma,2n)$ cross section. In Fig. 8, the solid bars indicated on some of the points give the statistical uncertainties in the data. The light extensions on these bars indicate the additional uncertainties resulting from the multiplicity correction.

The curve drawn in Fig. 8 has been calculated using the theory of Danos and Greiner. In calculating the eigenvalues and strengths of the various transitions the more exact expressions of Maximon[26] have been used. In this theory[27] the widths of the various peaks that go to make up the giant resonance have been shown to be given by an expression of the form

$$\Gamma=\Gamma_0 E^{\delta}. \tag{16}$$

Once the rotational energy parameter E_r and the energies of the beta and gamma vibrations, E_β and E_γ, have been determined from the low-energy spectra, the task of fitting the giant resonance reduces to the deter-

[25] P. Axel, J. Miller, C. Schuhl, G. Tamas, C. Tzara (to be published).
[26] L. C. Maximon (to be published).
[27] M. Danos and W. Greiner, Proceedings of the International Nuclear Physics Congress, Paris, 1964 (to be published).

TABLE I. Resonance parameters calculated for $\beta_0=0.30$, $\delta=2.0$, $E_r=23.35$ keV, $E_\gamma=771$ keV, $E_\beta=1460$ keV, and $E_m=14.3$ MeV.

$\lvert\Delta K\rvert$	S	n_2	E_n (MeV)	Γ_n (MeV)	σ_n (mb)
0	0	0	12.13	2.33	220
1	1	0	15.25	3.68	101
1	1	1	16.37	4.23	23
1	−1	0	17.21	4.65	122
1	−1	1	19.2	5.8	~0

mination of four adjustable parameters: the mean energy, E_m; the deformation parameter, β_0; the width, Γ_0; and the exponent, δ. The values used for these quantities for the curve given in Fig. 8 are listed in Table I with the resonance parameters for each of the transitions. The energies of the beta and gamma vibrations, E_β and E_γ, were taken from the low-lying spectra of Er^{166} as in the work of Danos and Greiner.[3]

In Figs. 5 and 7, the smooth curves have been calculated from the resonance parameters given in Table I. The quantities plotted represent, respectively,

$$\int_0^{E_i} \sigma_{1,2}' MN(E,E_i)dE \tag{17}$$

and

$$\frac{\int_0^{E_i} \sigma_{1,2}' MN(E,E_i)dE}{\int_0^{E_i} \sigma_{1,0}' MN(E,E_i)dE},$$

where $N(E,E_i)$ represents the bremsstrahlung spectrum, M the neutron multiplicity, and $\sigma_{1,2}'$ and $\sigma_{1,0}'$ are defined by Eq. (8c). In both figures the calculated curves have been normalized to the experimental data at the points indicated by the dot. Within the accuracy of the experiment there does not appear to be any serious discrepancy between the shapes of the calculated curves and the relative positions of the experimental points.

The curve given in Fig. 7 can be made absolute in the same sense the experimental measurements are absolute by using the appropriate constant indicated in Eq. (8a). The resulting normalization factor depends directly on the orientation parameter f_2. When this normalization is made, it is found that the calculated curve had to be multiplied by a factor of 0.82 ± 0.08 to bring it into agreement with the curve plotted in Fig. 7. The uncertainty given for this factor represents the largest it is felt reasonable to assign as a result of the estimated uncertainty in the parameter f_2.

The need for such a normalization factor may be an indication of the existence of a small additional scalar term in the holmium absorption cross section. Such a term would have none of the orientation effects of the type inherent in the hydrodynamic model of the nuclear photoeffect. It could be a term resulting from direct transitions from the ground state into the continuum. The addition of such a term in the absorption cross section would make it possible to greatly improve the quality of fit to the experimental data given in Fig. 8. The magnitude of the cross section required in both cases would correspond to a strength that is about 10–15% of the strength associated with the hydrodynamic model. A strength of this magnitude is quite consistent with the previous estimates of the magnitude of the direct photoeffect.[28]

ACKNOWLEDGMENTS

The authors want to acknowledge the many helpful discussions with M. Danos and W. Greiner. They are particularly indebted to L. C. Maximon for his help in the determination of the resonance parameters given in Table I. They also want to express their appreciation to H. Gerstenberg for his considerable help in taking and reducing the data and to R. S. Kaeser for valuable technical assistance. Special thanks are due A. Lopez and R. B. Dove for the many long hours they put in helping with the experiment as well as maintaining and operating the betatron and refrigeration system.

[28] L. B. Aull, G. C. Reinhardt and W. D. Whitehead, Nucl. Phys. **13**, 292 (1959).